

Optical and Magnetic Characteristics of Yttrium Doped ZnO Nanocrystalline Films

^{1,*} San-Lin Young, ¹ Hone-Zern Chen and ¹ Ming-Chen Kao

Abstract

Herein transparent $Zn_{1-x}Y_xO$ nanocrystalline films have been prepared on glass substrates by sol-gel spin coating method followed by thermal annealing treatment. The effects of yttrium doping on the microstructure, transmittance and magnetism of ZnO nanocrystalline films are investigated. The x-ray diffraction patterns of all compositions show the same wurtzite hexagonal structure with the space group $P6_3/mc$. FE-SEM images show uniform spherical grains of all $Zn_{1-x}Y_xO$ nanocrystalline films in which the grain size calculated by Debye-Scherrer's equation decreases progressively from 39.05 nm for $x=0$, 23.64 nm for $x=0.01$, to 18.79 nm for $x=0.02$. Red shift of the absorption edges is obtained from the optical transmittance spectra from 372 nm of undoped ZnO film to 367 nm of $Zn_{0.96}Y_{0.04}O$ film. The corresponding wide bandgap energy decreases slightly from 3.282 eV for $x=0$, 3.271 eV for $x=0.01$, to 3.266 eV for $x=0.02$. The saturation magnetization increases with the increase of Y concentration.

Keywords: ZnO, x-ray diffraction, Debye-Scherrer's equation, bandgap, magnetization.

*Corresponding Author: San-Lin Young
(E-mail: slyoung@hust.edu.tw)

¹Department of Electronic Engineering, Hsiuping University of Science and Technology, 11, Gongye Rd., Dali Dist., Taichung 41280, Taiwan.

1. Introduction

Wide band gap semiconductors have received much attention in recent years because of the application in short wavelength optical sensors, lasers and light emitting diodes. ZnO-based compound is one of the best candidates due to direct wide bandgap nature for UV photonic devices [1–2]. Not only does ZnO have similar physical and electrical properties as GaN, but also has a higher melting point and larger exciton binding energy than GaN. Companied with the recent development of nanotechnology, ZnO nanocrystalline films have offered a novel direction in the study of optoelectronics devices [3–6]. Progressive researches in the synthesis and characterization of the ZnO-based nanocrystalline films have been driven by the need to investigate high performance optoelectronic properties. ZnO film doped with selective elements offers an effective method to adjust the crucial properties for practical industrial applications [7–8].

ZnO crystal has been traditionally regarded as a nonmagnetic material. [9] However, some recent researches declared that ferromagnetism was observed from undoped nanostructured ZnO, which was suggested to be induced by defects [10–11]. Many further theoretical and experimental studies showed that ZnO doped with magnetic transition metal (TM) was a potential high-Curie-temperature

diluted magnetic semiconductor (DMS). The origin of the ferromagnetism of the ZnO-based DMS might be affected by the precipitates, clustering or secondary phase of doped magnetic elements [12]. Instead, ZnO-based DMS doped with non-magnet elements also offered an effective method to adjust the electrical, optical, and magnetic properties [13–14]. ZnO-based DMS has attracted broad interests for their possible use as spintronic materials [15–18]. ZnO nanostructures have been fabricated by various methods, such as thermal evaporation, metal–organic vapor phase epitaxy, and laser ablation within high vacuum or high temperature environment. Compared with the above mentioned processes, the sol–gel spin coating method provides a simple and low cost process to synthesize ZnO nanostructures.

In this work, we perform the simple fabrication method of $Zn_{1-x}Y_xO$ nanocrystalline films and study the substitution effect of Y for Zn on both optical and magnetic properties. Correlation between Y-doped induced defects and corresponding physical characteristics including optical and magnetic of the $Zn_{1-x}Y_xO$ nanocrystalline films is also systematically clarified in this approach.

2. Experimental Procedure

$Zn_{1-x}Y_xO$ ($x=0, 0.01$ and 0.02) nanocrystalline films were separately grown on glass substrates by the hydrothermal method. All glass substrates were ultrasonically cleaned in acetone, ethanol and water each for 10 min successively. Then glass substrates were dried by flowing nitrogen gas and 300°C heating. After the substrate cleaning processes, $Zn_{1-x}Y_xO$ nanocrystalline films were deposited on the

glass substrates by sol–gel spin coating method. [19] The source solutions were prepared by zinc acetate dehydrate $Zn(C_2H_3O_2)_2 \cdot 2H_2O$, yttrium (III) acetate tetrahydrate $Y_2(C_2H_3O_2)_3 \cdot 4H_2O$, 2-methoxyethanol $C_3H_8O_2$, and ethanolamine (2-aminoethanol) C_2H_7NO . Zinc acetate dehydrate and yttrium (III) acetate tetrahydrate were first dissolved in 2-methoxyethanol with stoichiometric proportions. The concentration of metal ions was kept at 0.5 M. Then ethanolamine was added into the solutions to form stable precursor solutions. After stirring at 150°C for 1 h on a hotplate, transparent solutions were obtained. Then the $Zn_{1-x}Y_xO$ thin films were separately grown on the cleaned glass substrates. Firstly, the precursor solutions were dropped on the glass substrates and spun at 2500 rpm for 30 sec. Then the substrates were in the following heated on a hot-plate at 300°C for 2 min. The deposited processes were repeated for ten times, respectively. Finally, the samples were annealed in air by a tube furnace for thermal annealing treatment at 500°C for 3 hours.

The crystal structure and grain orientation of ZnO films were determined by the x-ray diffraction (XRD) patterns using a Rigaku D/max 2200 x-ray diffractometer with Cu–K α radiation. The XRD data were recorded at room temperature under the 2θ ranges from 20° to 60° with a step width of 0.01° and a scan speed of $0.5^\circ/\text{min}$. Morphological characterization was observed using a field emission scanning electron microscopy (FE-SEM, JEOL JSM-6700F) at 3.0 kV. The transmittance spectra in the wave length between 300 and 800 nm were obtained by JASCO V–670 spectrophotometer. Room temperature photoluminescence (RTPL) spectroscopy was used to measure optical emissions from 350 to

645 nm by a He–Cd laser with the wavelength of 325 nm. The magnetization measurements were performed between –5 and 5 kOe by a MicroMag 2900 alternative gradient magnetometer at room temperature to investigate the magnetic properties of $Zn_{1-x}Y_xO$ nanorods.

3. Results and Discussion

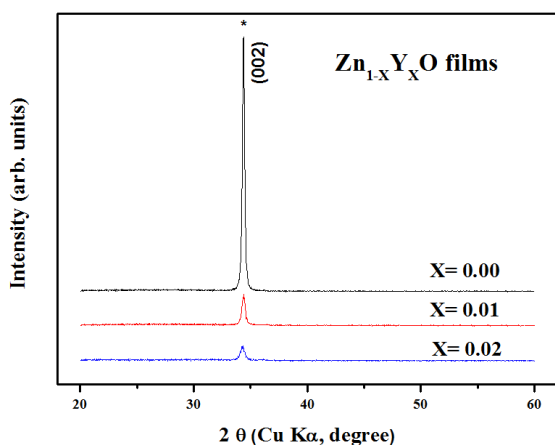


Figure 1: X-ray diffraction patterns of $Zn_{1-x}Y_xO$ nanocrystalline films grown on glass substrate heating at 500°C.

Figure 1 illustrates the XRD patterns of undoped ZnO and Y-doped nanocrystalline films. Based on the XRD patterns, all Y-doped samples are found to have the same single polycrystalline phase with the wurtzite hexagonal structure of P63/mc as undoped ZnO film does. All samples exhibit the (002) preferred orientation, indicating that they are c-axis oriented. The progressively broadening of the XRD peaks with the increase of Y concentration is related to the decrease of the grain size of the nanocrystalline films. The average grain size of the samples obtained by the classical Debye–Scherrer's equation decreases progressively from 39.05 nm for $x=0$, 23.64 nm for $x=0.01$, to 18.79 nm for $x=0.02$.

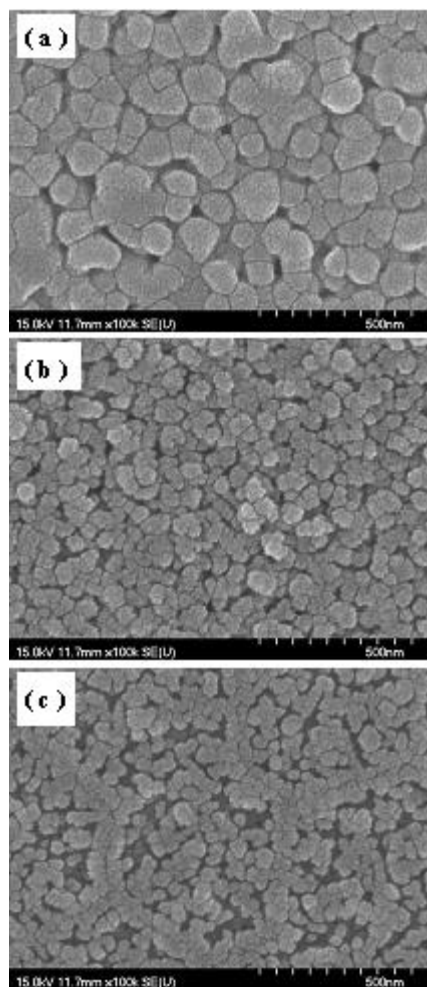


Figure 2: SEM images of $Zn_{1-x}Y_xO$ nanocrystalline films with (a) $x=0.00$ (b) $x=0.01$, and (c) $x=0.02$. The bars denote 500 nm.

Surface morphology of FE-SEM images shown in Fig. 2 reveals granular nanocrystalline structure for all $Zn_{1-x}Y_xO$ films. It is clear that the grain size decreases progressively with the increase of the Y concentration, which is consistent with the results indicated in Fig. 1.

The transmittance spectra of $Zn_{1-x}Y_xO$ thin films are measured as a function of wave length in the range of 300–800 nm as shown in Fig. 3. Red shift of the absorption edges is obtained from the optical transmittance spectra from 372 nm of undoped ZnO film to 377 nm of $Zn_{0.98}Y_{0.02}O$ film. All $Zn_{1-x}Y_xO$

films exhibit good visible light transmittance. The band gaps of these films are determined by means of a graphical method from the absorption coefficient derived from the transmittance results. The absorption coefficient obeys the relationship,

$$\alpha h\nu = A(h\nu - E_g)^n, \quad (1)$$

where A is a constant, h is the Planck's constant, ν is the photon frequency, E_g is the band gap and $n=1/2$ for direct semiconductor. The band gaps of all samples are evaluated by extrapolating the straight line portion of the curve at $(\alpha h\nu)^2=0$ as shown in the Fig. 4. The calculated value of the corresponding bandgap energy decreases slightly from 3.282 eV for $x=0$, 3.271 eV for $x=0.01$, to 3.266 eV for $x=0.02$. The $Zn_{1-x}Y_xO$ films are found to have a lower band gap with higher dopant concentration. The reason of the decrease of band gap with the increase of x is attributed to both the decrease of crystalline size and the modification of the grain boundary configuration during growth.

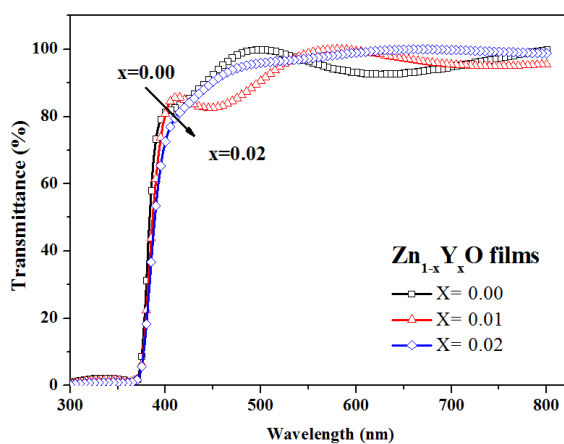


Figure 3: Optical transmission spectra of $Zn_{1-x}Y_xO$ films.

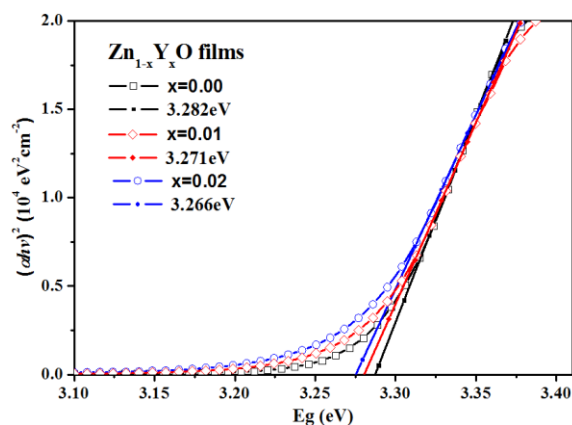


Figure 4: $(\alpha h\nu)^2$ vs energy gap curves of $Zn_{1-x}Y_xO$ nanocrystalline films.

The magnetization curve measurements are performed using an AGM with an external magnetic field between -5 kOe and 5 kOe at room temperature. As shown in Fig. 5, results of magnetic characterization obviously show ferromagnetic behavior for all $Zn_{1-x}Y_xO$ nanocrystalline films. Besides, the increase of saturation magnetization is obtained from 0.311 emu/g for $x=0$, 0.277 emu/g for $x=0.01$, to 0.169 emu/g for $x=0.02$. As can be observed, the curves rise sharply as the concentration of Y increases, which indicates the films are easy to be magnetized by an external magnetic field with the increase of Y doping concentration.

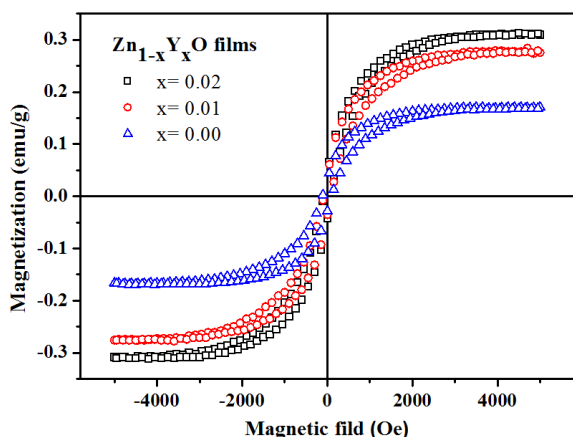


Figure 5: Hysteresis loops of $Zn_{1-x}Y_xO$ nanocrystalline films measured at room temperature.

4. Conclusions

$Zn_{1-x}Y_xO$ nanocrystalline films have been separately deposited on glass substrates by a sol-gel spin coating method. The correlation between the Y doping concentration and their microstructural, and optical and magnetic properties are studied in details. XRD patterns show that all films are found to exhibit the same polycrystalline phase with the wurtzite hexagonal structure of group space P63/mc. FE-SEM Surface images show the grain size and the bandgap of the $Zn_{1-x}Y_xO$ nanocrystalline films decreases with the increase of Y concentration. Besides, the saturation magnetization of the $Zn_{1-x}Y_xO$ nanocrystalline films increases with the increase of Y doping concentration.

Acknowledgment

This work was sponsored by the Ministry of Science and Technology of the Republic of China under the grant Nos. MOST 103-2221-E-164-003 and MOST 102-2112-M-164-001-MY2.

References

- [1]. J. R. Sadaf, M. Q. Israr, S. Kishwar, O. Nur, and M. Willander: *Nanoscale Res. Lett.* 5 (2010) 957.
- [2]. S. Dhara and P. K. Giri: *Nanoscale Res. Lett.* 6 (2011) 504.
- [3]. W. Guo, Y. Yang, J. Qi, J. Zhao, and Y. Zhang: *Appl. Phys. Lett.* 97 (2010) 133112.
- [4]. V. Chivukula, D. Ciplys, M. Shur, and P. Dutta: *Appl. Phys. Lett.* 96 (2010) 233512.
- [5]. C.-H. Chen, S.-J. Chang, S.-P. Chang, M.-J. Li, I.-C. Chen, T.-J. Hsueh, and C.-L. Hsu: *Appl. Phys. Lett.* 95 (2009) 223101.
- [6]. M. A. Zimmerler, T. Voss, C. Ronning, and F. Capasso: *Appl. Phys. Lett.* 94 (2009) 241120.
- [7]. N. Ito, Y. Sato, P. K. Song, A. Kaijio, K. Inoue, and Y. Shigesato: *Thin Solid Films* 496 (2006) 99.
- [8]. T. F. Chung, L. B. Luo, Z. B. He, Y. H. Leung, I. Shafiq, Z. Q. Yao, and S. T. Lee: *Appl. Phys. Lett.* 91 (2007) 233112.
- [9]. M. D. McCluskey and S. J. Jokela: *J. Appl. Phys.* 106 (2009) 071101.
- [10]. G. Xing, D. Wang, J. Yi, L. Yang, M. Gao, M. He, J. Yang, J. Ding, T. C. Sum, and T. Wu: *Appl. Phys. Lett.* 96 (2010) 112511.
- [11]. S. Ghosh, G. G. Khan, and K. Mandal: *EPJ Web Conf.* 40 (2013) 03001.
- [12]. T. Li, H. Fan, J. Yi, T. S. Heng, Y. Ma, X. Huang, J. Xue, and J. Ding: *J. Mater. Chem.* 20 (2010) 5756.
- [13]. L. Li, S. Pan, X. Dou, Y. Zhu, X. Huang, Y. Yang, G. Li, and L. Zhang: *J. Phys. Chem. C* 111 (2007) 7288.

- [14]. C. Cheng, G. Xu, H. Zhang, Y. Luo, and Y. Li: Mater. Lett. 62 (2008) 3733.
- [15]. S. Gupta, W. E. Fenwick, A. Melton, T. Zaidi, H. Yu, V. Rengarajan, J. Nause, A. Ougazzaden, and I. T. Ferguson: J. Cryst. Growth 310 (2008) 5032.
- [16]. A. Fouchet, W. Prellier, and L. Mechin: Superlattices Microstruct. 42 (2007) 185.
- [17]. D. P. Joseph, G. S. Kumar, and C. Venkateswaran: Mater. Lett. 59 (2005) 2720.
- [18]. N. Kouklin, M. Omari, A. Gupta, and S. Sen: J. Electron. Mater. 38 (2009) 596.
- [19]. S. A. Kamaruddin, K.-Y. Chan, H.-K. Yow, M. Z. Sahdan, H. Saim, and D. Knipp: Appl. Phys. A 104 (2011) 263.



San-Lin Young was born in Taichung, Taiwan, in 1964. He received the Ph.D. degrees from National Sun Yat-sen University, Kaohsiung, Taiwan, in 2002. He

worked on the synthesis and characterization of the nanostructure materials and photonic devices funded by the National Science Council of the Republic of China for the past ten years. Currently, he is a full professor at the Department of Electronic Engineering, Hsiuping University of Science and Technology.



Hone-Zern Chen was born in Changhua, Taiwan, on August 29, 1959. He received the M.S. and Ph.D. degrees in electrical engineering from National Sun

Yat-Sen University in 1990 and 1996, respectively. His current research interests are in the areas of electroceramics, ferroelectric, and magnetic materials. Currently, he is a full professor at the Department of Electronic Engineering, Hsiuping University of Science and Technology.



Ming-Chen Kao was born in Changhua, Taiwan, R.O.C. on October 22, 1976. He received the M.S. and Ph.D. degrees in electrical engineering from National Sun Yat-Sen University in 2000 and 2004, respectively. His current research interests are in the areas of ferroelectric materials and dye-sensitized solar cell. Currently, he is a full professor at the Department of Electronic Engineering, Hsiuping University of Science and Technology.